11-23-2016

Influence of Tick and Mammalian Physiological Temperatures on Borrelia Burgdorferi Biofilms

Shafiq Shaikh
University of New Haven

Venkata Arun Timmaraju
University of New Haven

Jason Torres
University of New Haven

Kayla Socarras
University of New Haven

Priyanka A. Theophilus
University of New Haven

See next page for additional authors

Publisher Citation

Shaikh, S., Timmaraju, V. A., Torres, J. P., Socarras, K. M., Theophilus, P. A., & Sapi, E. (2016). Influence of tick and mammalian physiological temperatures on Borrelia burgdorferi biofilms. Microbiology, 162(11), 1984-1995.

Comments

This is the authors' accepted version of the article published in the journal *Microbiology*. The version of record may be found at the Microbiology Society web site via http:dx.doi.org/10.1099/mic.0.000380

Microbiology

Influence of tick and mammalian physiological temperatures on Borrelia burgdorferi biofilms

--Manuscript Draft--

Manuscript Number:	MIC-D-16-00134R1
Full Title:	Influence of tick and mammalian physiological temperatures on Borrelia burgdorferi biofilms
Short Title:	Borrelia biofilm phenotypes at 23ºC, 33ºC and 37ºC
Article Type:	Standard
Section/Category:	Physiology and metabolism
Corresponding Author:	Shafiq Shaikh, BTech, MS Yale University School of Medicine new haven, connecticut UNITED STATES
First Author:	Shafiq Shaikh, BTech, MS
Order of Authors:	Shafiq Shaikh, BTech, MS
	Venkata Arun Timmaraju, BSC, PGD, MS
	Jason P Torres, BS
	Kayla M Socarras, BS, MS
	Priyanka A.S. Theophilus, BTech, MS, MS
	Eva Sapi, Phd
Abstract:	The spirochete bacterium Borrelia burgdorferi sensu lato is the etiologic agent of Lyme disease. Borrelia is transmitted to mammals through tick bite and is adapted to survive at tick and mammalian physiological temperatures. We have previously shown that B. burgdorferi can exist in different morphological forms including an antibiotic resistant form called biofilms both in vitro and in vivo. B. burgdorferi forms aggregates in ticks as well as in humans, indicating potential of biofilm formation at both 23ºC and 37ºC. However, the role of various environmental factors that influence Borrelia biofilm formation are yet unknown. In this study, we investigated the effect of tick (23ºC), mammalian physiological (37ºC) and standard in vitro culture temperature (33ºC) with the objective of elucidating the effect of temperature on Borrelia biofilm phenotypes in vitro using two B. burgdorferi sensu stricto strains (B31, and 297). Our findings show increased biofilm quantity, biofilm size, exopolysaccharide content and enhanced adherence as well as reduced free spirochetes at 37ºC for both strains, when compared to growth at 23ºC and 33ºC. There were no significant variations in the biofilm nanotopography and the type of extracellular polymeric substance in Borrelia biofilms formed at all three temperatures. Significant variations in extracellular DNA content were observed in the biofilms of both strains cultured at the three temperatures. Our results indicate that temperature is an important regulator of Borrelia biofilm development and the mammalian physiological temperature favours increased biofilm formation in vitro compared to tick physiological temperature and in vitro culture temperature.

Influence of tick and mammalian physiological temperatures on *Borrelia burgdorferi* biofilms

Shafiq Shaikh [1, 2], Venkata Arun Timmaraju [1,3], Jason P. Torres [1], Kayla M. Socarras [1], Priyanka A. S. Theophilus [1, 4], Eva Sapi*[1]

[1] Lyme Disease Research Group, 300 Boston Post Road, University of New Haven, West Haven, CT, 06516

[2] Present address: Department of Obstetrics, Gynecology & Reproductive Sciences, Yale School of Medicine, New Haven, CT, USA

[3] Present address: Interpace Diagnostics, New Haven, CT, USA

[4] Present address: Department of Microbiology and Immunology, East Carolina University, Greenville, NC, USA

∗Corresponding author: Lyme Disease Research Group, 300 Boston Post Road, University of New Haven, West Haven, CT, 06516, USA. Tel: 203-479-4552.

E-mail: esapi@newhaven.edu

Running title: *Borrelia* biofilm phenotypes at 23 and 37°C

Keywords: *Borrelia burgdorferi*, Lyme disease, EPS, AFM, Biofilm phenotype, Persisters

Abstract

The spirochete bacterium *Borrelia burgdorferi* sensu lato is the etiologic agent of Lyme disease. *Borrelia* is transmitted to mammals through tick bite and is adapted to survive at tick and mammalian physiological temperatures. We have previously shown that *B. burgdorferi* can exist in different morphological forms including an antibiotic resistant form called biofilms both *in vitro* and *in vivo*. *B. burgdorferi* forms aggregates in ticks as well as in humans, indicating potential of biofilm formation at both 23°C and 37°C. However, the role of various environmental factors that influence *Borrelia* biofilm formation are yet unknown. In this study, we investigated the effect of tick (23°C), mammalian physiological (37°C) and standard in vitro culture temperature (33°C) with the objective of elucidating the effect of temperature on *Borrelia* biofilm phenotypes *in vitro* using two *B. burgdorferi* sensu stricto strains (B31, and 297). Our findings show increased biofilm quantity, biofilm size, exopolysaccharide content and enhanced adherence as well as reduced free spirochetes at 37°C for both strains, when compared to growth at 23°C and 33°C. There were no significant variations in the biofilm nanotopography and the type of extracellular polymeric substance in *Borrelia* biofilms formed at all three temperatures. Significant variations in extracellular DNA content were observed in the biofilms of both strains cultured at the three temperatures. Our results indicate that temperature is an important regulator of *Borrelia* biofilm development and the mammalian physiological temperature favours increased biofilm formation *in vitro* compared to tick physiological temperature and *in vitro* culture temperature.

Introduction

With approximately 300,000 new cases reported by Center for Disease Control (CDC), Lyme disease is the most common vector borne illness in the United States (Gomes-Solecki, 2014). Lyme disease is caused by the pleomorphic spirochete *B. burgdorferi* and is transmitted to humans and vertebrates through the bite of *Ixodes* tick (Wang *et al.*, 1999; Rudenko et al., 2011 ; Brisson et al., 2010).

B. burgdorferi has been observed in different morphological forms such as spherical cyst-like form (Al-Robaiy *et al.*, 2010 ; Alban *et al.*, 2000 ; Miklossy *et al.*, 2008), detaching pearl-like or granular structures (Aberer & Duray, 1991 ; Garon *et al.*, 1989 ; Barbour & Hayes, 1986) and aggregates (Srivastava & de Silva, 2009 ; Sapi *et al*., 2012). Recently, we and others have shown that *B. burgdorferi* forms biofilms or aggregates *in vitro* and *in vivo* (Sapi *et al*., 2012 ; Sapi *et al*., 2016 ; Timmaraju *et al*., 2015 ; Merilainen *et al.*, 2015) as well as highly drug resistant persisters (Embers *et al.*, 2012 ; Theophilus *et al.*, 2015 ; Feng et al., 2014).

Bacterial biofilms are conglomerates of planktonic organisms characterized by the presence of a rich extracellular polymeric substance (EPS) which shield constituent individuals (including persisters) from adverse environmental conditions (Flemming and Wingender 2010 ; O'Toole *et al*., 2000 ; Stewart & Franklin, 2008). Biofilms are highly resistant antimicrobial agents and are very difficult to eradicate, thereby contributing towards chronicity of the infections (Lewis, 2007 ; Sapi *et al*., 2011; Høiby *et al*., 2010).

EPS plays major role in biofilm development (initial substrate adhesion), maturation (rigidity and structure) and protection (antibiotic resistance) (Sutherland, 2001; Vu et al., 2009). Temperature is a major environmental factor that regulates EPS production, thereby determining biofilm phenotypes in various bacteria such as *Yersinia pestis, Listeria monocytogens, Staphylococus aeureus* and *Enterococcus faecium* (Czaczyk & Myszka, 2007 ; Hinnebusch & Erickson, 2008 ; Yoong *et al*., 2012 ; Di Bonaventura *et al*., 2008 ; Ochiai *et al*., 2014 ; Obana *et al*., 2014).

B. burgdorferi is adapted to survival in multiple hosts and infects humans and mice, whose physiological temperature is 37^0C, whereas its vector, the *Ixodes scapularis* tick has a physiological temperature of 23^0C. *B. burgdorferi* forms aggregates, in both ticks and humans, indicating potential biofilm formation at both 23^0C and 37^0C (Sapi *et al.*, 2016 ; Dunham-Ems *et al.*, 2009).

Interestingly, the tick-human life cycle of *B. burgdorferi* parallels the flea-human life cycle of *Y. pestis*, the bubonic plague causative bacterium. *Y. pestis* forms attached biofilms in the flea foregut and is transmitted to the mammalian host through biofilms (Hinnebusch & Erickson, 2008). Also, in *Y. pestis* biofilms, the expression of a major EPS polysaccharide poly-N-acetyl glucosamine differs between the mammalian temperature of 37°C compared to the flea temperature of 28°C (Yoong *et al.*, 2012). Studying *B. burgdorferi* biofilm formation at tick and mammalian physiological temperatures (23°C and 37°C, respectively), as well as *in vitro* culture temperature (33°C) may shed light on biofilm development, morphology and EPS characteristics, and lead to a better understanding of *Borrelia* biofilm life cycle.

In this study, we analyzed the role of tick and mammalian physiological temperatures in determining the biofilm phenotypes of two wild type *B. burgdorferi* strains, adapted to growth in ticks and mammals - strain B31 isolated from tick *Ixodes dammini* and strain 297 isolated from human cerebrospinal fluid (Johnson *et al*., 1984). Using comprehensive cell-based assays and atomic force microscopy, we found that the mammalian physiological temperature 37^0C (*in vitro*) provides a suitable niche favouring increased biofilm formation by *B. burgdorferi*.

Materials and methods

Bacterial strains and culture conditions

Low passage isolates of *Borrelia burgdorferi* B31 strain (ATCC # 35210) and *Borrelia burgdorferi* strain 297 (ATCC # 53899), were cultured in BSK-H media (Sigma) supplemented with 6% rabbit serum (Pel-Freeze) in 15 ml sterile glass tubes at 33^0C and 5% CO2 without any antibiotics. The B31 strain was isolated from tick *Ixodes dammini* and strain 297 was isolated from human cerebrospinal fluid (Johnson et al., 1984). For biofilm formation, *Borrelia* spirochetes (500,000) were seeded onto 4-well Permanox chamber (Lab-Tek II) or glass chamber slides (Thermo Scientific) or 48-well cell culture plates (Corning) and cultured at 23^0C, 33^0C or 37^0C at 5% CO2 without antibiotics for 7 days, as described previously (Sapi et al., 2012).

Biofilm coverage estimation

Culture media from the 4-well Permanox chamber slide cultures were removed and five random phase contrast micrographs per well for three wells for each temperature (n=9) were captured for the adherent biofilms using Axio Observer A1 microscope ™ (Zeiss). Image J software (Rasband, W.S., ImageJ, U. S. National Institutes of Health, Bethesda, Maryland, USA, http://imagej.nih.gov/ij/) was used for image analysis. Image scale was calibrated using the set scale tool in the analyze menu. The phase contrast images were processed for mean biofilm coverage area and mean individual biofilm area by coloring the boundaries of the biofilm through the paint tool. The colored boundaries were then selected for analysis using the threshold tool in the image menu. After the boundaries were selected, the area enclosed by the boundaries was then analyzed through the analyze particles tool in the analyze menu by checking the option "include holes".

Atomic force microscopy

Contact mode atomic force microscopy was performed on *Borrelia* biofilms using a Nanosurf Easyscan 2 Flex AFM with SHOCONG probes (AppNANO™) as previously described (Timmaraju *et al.*, 2015). Biofilms were scanned at a constant force mode by scanning 256 points per line using 10.3nN set point with P gain of 1200, I gain of 300 and D gain of zero. The scans obtained were processed using Gwyddion (http://gwyddion.net/). Mean biofilm height was obtained by scanning 4 different biofilms for each strain at the three different temperatures (n=4).

EPS staining

EPS staining was performed as previously described, using a mannose specific HHA lectin (495 nm) and an alginate specific antibody (594 nm) (Sapi *et al.*, 2012 ; Timmaraju *et al.*, 2015). Fluorescent micrographs of the biofilms were captured with Leica DM2500 microscope at 400X.

Alginate and HHA lectin specificity was verified by inhibiting Alginate antibody with 0.05M sodium alginate and HHA lectin with 0.5 M mannose prior to incubation with biofilms.

Extracellular DNA staining and quantification

Borrelia spirochetes were cultured for 7 days on a 48 well cell culture plate (Corning) to initiate biofilm formation. Culture media was removed and 150µl of TE SYBR green (1:400 in TE buffer) was added to the wells. The plates were then shaken at 150 rpm for 15 min and fluorescence intensity was measured at excitation 485nm / emission 528nm (n=3). Lambda DNA (Invitrogen™, Molecular probes) was used to generate eDNA standards (n=2) at concentrations 31.25µg/ml, 28.75µg/ml, 26.25µg/ml, 23.75µg/ml, 21.25µg/ml, 18.75µg/ml, 16.25µg/ml and 13.75µg/ml [Supplementary fig. S3]. Raw fluorescence intensity values were interpolated into eDNA concentrations using GraphPad Prism 6 (GraphPad Software, La Jolla California USA, www.graphpad.com). eDNA staining of the biofilm was obtained by adding 200µl of SYBR green (1:400 in TE buffer) to the biofilm culture. The cell culture plate was incubated for 5 min and the culture media was removed. Fluorescent micrographs of the biofilms were acquired using ZOE fluorescent cell imager (Biorad) at 200X. Extracellular DNA content in the biofilms was divided by the log transformed mean biofilm coverage area (μm^2) and the ratio was expressed as the content of extracellular DNA (eDNA) in the biofilm per μm^2 of the biofilm ($\mu g/\mu m^2$).

Free spirochete counting

Borrelia spirochetes after 7 days of culture were stained with SYBR Green dye (497 nm) (Thermo Fisher) and fluorescent micrographs were acquired using Leica DM2500 fluorescence microscope at 200X, scale bar = 100µm. Free *Borrelia* spirochetes (unstained) in the culture were counted by taking two microliter of culture from 4-well chambers slides at different temperatures, followed by counting the spirochetes in 5 different grids on a Petroff-Hausser chamber (Hausser Scientific) using dark field microscopy (n=9). The data was log transformed and the mean number of spirochetes per grid were analyzed.

Total carbohydrate assay

B. burgdorferi spirochetes were cultured as described above to initiate biofilm formation on 48-well cell culture plates (Corning). The media was removed and the adherent biofilms were scraped from the wells (n=9) with PBS, pH 7.4. The mixture was then centrifuged at 1650 g for 5 min to pellet the biofilm. The supernatant was discarded and the biofilms were then resuspended in 200 µl deionized water. One hundred microliters of 5% phenol (Fisher) and 500 µl of 100% sulfuric acid (Fisher) were added to the mix. The plate was then incubated in dark for 20 min at room temperature before reading the absorbance at 485 nm. Carbohydrate standards were generated by performing total carbohydrate assay on glucose concentrations of 16 mg/ml, 8 mg/ml, 4 mg/ml, 2 mg/ml, 1 mg/ml, 0.5 mg/ml, 0.25mg/m, 0.125 mg/ml and 0.0625 mg/ml [Supplementary fig. S2]. The total carbohydrate content of the biofilms (mg/ml) were interpolated from the carbohydrate standards using GraphPad Prism 6 (GraphPad Software, La Jolla California USA, www.graphpad.com). Carbohydrate content in the biofilms (µg) cultured at the three temperatures was divided by log transformed mean biofilm coverage area (μm^2). The ratio was expressed as the content of carbohydrates present in the biofilm per μm^2 of the biofilm ($\mu g/\mu m^2$).

Biofilm adherence assay

B. burgdorferi spirochetes were cultured as described above to initiate biofilm formation on 48-well cell culture plates (Corning). To determine the adherence of the biofilms, shaking technique was used (Srere, 1973 ; Dutta & Willcox, 2013 ; Katsikogianni & Missirlis, 2004). Briefly, after 7 days of culturing, 3 random phase contrast micrographs were taken for each well containing biofilms as well as culture media for each temperature. Then the plates were shaken at 60 rpm for 10 sec on a horizontal orbital shaker. The culture media was removed and 3 additional random phase contrast micrographs were taken for all the wells (n=9) for each temperature containing only adherent biofilms. The number of biofilms per a field of view were counted and averaged before and after shaking and the data was presented as a percentage.

Statistical analysis

All the statistical analysis was performed using GraphPad Prism 6 (GraphPad Software, La Jolla California USA, www.graphpad.com). At least three independent measurements were made for all experiments, and the raw data was represented as mean ± standard deviation, data was Log transformed where indicated. Two-way analysis of variance (ANOVA) was performed using uncorrected Fisher LSD multiple comparison test, with $P<0.05$ to determine significant differences between datasets.

Results

In this study, we performed a multi-parametric assessment to address three major questions: 1) What is the influence of mammalian and tick physiological temperatures on biofilm phenotypes of *B. burgdorferi*? 2) Are there any strain specific phenotypic differences between the B31 and 297 strains? 3) Does a potential relationship exist between the biofilm EPS and temperature?

Decrease in the number of free spirochetes and increased adherence of biofilms after 7 days of culture at 37^{0}C

To analyze whether the increased biofilm formation was potentially due to the conversion of spirochetes to biofilms, we performed two sets of experiments. First, we assessed the planktonic spirochetes in culture after 7 days of culture by performing direct cell counts of spirochete cultures grown at 23^{0}C, 33^{0}C or 37^{0}C (n=9). We observed significantly fewer free spirochetes in the culture of B31 and 297 strains maintained at 37^{0}C when compared to cultures at 23^{0}C and 33^{0}C [$p<0.01$, Fig. 1 (a and d)].

Having observed lower spirochete counts at 37^{0}C, we next wanted to determine whether 37^{0}C promotes surface adherence of *Borrelia* biofilms. After culturing the biofilms for 7 days, we observed a significant increase in biofilm adhesion at 37^{0}C when compared to 23^{0}C and 33^{0}C (n=9) for strains B31 and 297 [$P<0.0001$, Fig. 1 (a and c)]. Biofilms of strain 297 had significantly enhanced biofilm adhesion at 23^{0}C, 33^{0}C or 37^{0}C when compared to biofilms of strain B31 [$P<0.05$ for 23^{0}C, 33^{0}C and $P<0.0001$ for 37^{0}C, Fig. 1 (b)].

Increased biofilm formation and biofilm sizes by *B. burgdorferi* at 37^{0}C

To assess the effect of different temperatures on biofilm formation and organization, *B. burgdorferi* strains B31 and 297 were cultured at 23^{0}C, 33^{0}C or 37^{0}C for 7 days. Both strains formed biofilms at all three temperatures and a significant increase in biofilm formation was observed at 37^{0}C [Fig. 2(a-f)]. To measure the amount of biofilms formed at different temperatures, the mean biofilm coverage area was analyzed per field of view. Strain B31 showed significantly higher mean biofilm coverage area at 37^{0}C in comparison to biofilms formed at 23^{0}C and 33^{0}C [$P<0.01$, Fig. 2(g)] (n=9). Strain 297 similarly demonstrated increased biofilm coverage area at 37^{0}C when compared to biofilms formed at 23^{0}C and 33^{0}C [$P<0.01$, Fig. 2(g)] (n=9). Furthermore, *B. burgdorferi* strain B31 showed significantly higher biofilm formation ($P<0.01$) at 37^{0}C when compared to strain 297 [Fig. 2(g)] (n=9).

To assess whether temperature also affects size of individual biofilm, we analyzed the mean area occupied by individual biofilms. Both strains produced biofilms with significantly larger individual biofilms at 37^{0}C when compared to biofilms at 23^{0}C and 33^{0}C [$P<0.01$, Fig. 2(h)] (n=9). Biofilms of strain B31 cultured at 37^{0}C showed significantly larger individual biofilms when compared to biofilms of strain 297 cultured at the same temperature [$P<0.01$, Fig. 2(h)] (n=9).

3D nano-morphology and topography of *Borrelia* biofilms at different temperatures

In the next set of experiments, we analyzed whether temperature could affect the structural organization of the biofilms. We investigated the nano-morphology and topography of the biofilms by employing contact-mode atomic force microscopy as previously described (Sapi *et al*., 2012 ; Obana et al., 2014 ; Hinthong et al., 2015 ; Timmaraju *et al.*, 2015). We found that the biofilms formed by both strains at the three temperatures have the characteristic "tower morphology" of *B. burgdorferi* as previously described [Fig. 3(a, b)] (Sapi *et al.*, 2012 ; Timmaraju et al., 2015). In order to assess any potential differences in the topography and heights of the towers, four random biofilms for each strain at the three temperatures were scanned (n=4). Differences in the height of the biofilms (topography) was analyzed using two-way ANOVA [Fig 4]. No significant differences were observed in the topography and the mean height, with the biofilms of strains B31 and 297 at 23^0C, 33^0C or 37^0C [Fig. 3(a, b), $p>0.05$,] showing similar topography and no significant difference in the height of the biofilm towers.

EPS characteristics of biofilms and increased carbohydrate content in *Borrelia* biofilms at 37^0C

To assess the effect of temperature on EPS composition and to investigate whether the biofilm markers alginate and mannose are expressed in biofilms at all three temperatures, we immunostained *B. burgdorferi* biofilms with alginate antibody and mannose specific HHA lectin. The staining of *B. burgdorferi* biofilms with an alginate specific antibody showed the presence of alginate for B31 and 297 biofilms [Fig. 5(a)] at 23^0C, 33^0C or 37^0C respectively, as observed previously in B31 biofilms (Sapi *et al.*, 2012). Mannose specific HHA lectin staining of the biofilms showed the presence of mannose for B31 -and 297 biofilms [Fig. 5(b)] at 23^0C, 33^0C or 37^0C respectively as previously observed (Timmaraju *et al.*, 2015). The specificity of alginate and HHA lectin staining was demonstrated by inhibiting the alginate antibody and HHA lectin with 0.05M sodium alginate and 0.25M mannose respectively [Fig. S1]. To quantify the effect of temperature on EPS production, we performed total carbohydrate assay (TCA). We observed a significant increase in the amount of carbohydrate (µg) present in the biofilms cultured at 37^0C when compared to biofilms at 23^0C [$P<0.01$, Fig. 5(c)] (n=9) and 33^0C [$P<0.05$, Fig. 5(c)] for strain 297(n=9). Furthermore, biofilms of strain B31 formed at 37^0C [$P<0.01$, Fig. 5(c)] (n=9) and 33^0C [$P<0.05$, Fig. 5(c)] (n=9) showed increased carbohydrate content when compared to 23^0C. Strain 297 demonstrated higher content of carbohydrates per μm^2 in biofilms cultured at 37^0C in comparison to biofilms cultured at 23^0C [$P<0.01$, Fig. 5(d)] (n=9) and 33^0C [$P<0.05$, Fig. 5(d)] (n=9). Moreover, biofilms of strain B31 showed reduced carbohydrate content per μm^2 when cultured at 23^0C compared to 33^0C [$P<0.05$, Fig. 5(d)] (n=9) and 37^0C [$P<0.01$, Fig. 5(d)] (n=9).

Extracellular DNA content in *Borrelia* biofilms at 23^0C, 33^0C or 37^0C

Borrelia biofilms after 7 days of culture were stained with SYBR green to quantitate and to visualize the extracellular DNA in the biofilm. There was a significant increase in the extracellular DNA content in the biofilms of strain 297 at 37^0C compared to 23^0C and 33^0C [$P<0.05$, Fig. 6(b)] (n=3). However, no significant difference in extracellular DNA content was observed in biofilms of strain B31 at 23^0C, 33^0C or 37^0C [Fig. 6(a, b)] (n=3). Biofilms of strain 297 showed no significant differences in the content of extracellular DNA (µg) present per μm^2 of the biofilms ($\mu g/\mu m^2$) cultured at the three temperatures [Fig. 6(a, c)] (n=3). However, biofilms of strain B31

cultured at 37^0C showed reduced extracellular DNA content present per μm^2 of the biofilm ($\mu g/\mu m^2$) compared to 33^0C [P<0.05, Fig. 6(c)] (n=3).

Discussion

The goal of this study was to investigate *Borrelia* biofilm formation at 23°C and 37°C *in vitro* in addition to 33°C as reported previously (Sapi *et al.*, 2012). Our findings demonstrated that mammalian physiological temperature of 37°C increases *B. burgdorferi* biofilm formation, biofilm sizes and EPS production compared to the tick physiological temperature of 23°C and *in vitro* culture temperature 33°C. These findings are consistent with observations from various biofilm forming bacteria such as *Streptococcus intermedius*, *Listeria monocytogenes*, *Yersinia pestis*, *Staphylococcus aureus and Salmonella spp* where temperature has been demonstrated to influence biofilm formation (Ahmed et al., 2008 ; Di Bonaventura et al., 2008 ; Yoong et al., 2012 ; Stepanović *et al.*, 2003 ; da Silva Meira *et al.*, 2012). Bacteria such as *Aeromonas caviae* have enhanced biofilm formation *in vitro* at 28°C, which is also close to the temperature *Aeromonas caviae* grows in the nature (Angeles-morales *et al.*, 2012). Interestingly, *B. burgdorferi* in nature is found in both tick and in mammals with physiological temperatures of 23°C and 37°C, and has demonstrated biofilm or aggregate formation in both (Sapi *et al.*, 2016 ; Dunham-Ems *et al.*, 2009). In this study, we show that *Borrelia* forms biofilms at both 23°C and 37°C *in vitro*. Additionally, we show that temperature can modulate several phenotypic characteristics of the biofilm such as biofilm size, amount of extracellular polysaccharides, extracellular DNA content within the biofilm and biofilm adhesion. Apart from phenotypic variation found in the biofilms cultured at three different temperatures, we also observed reduced spirochete numbers at 37°C compared to 23°C and 33°C. It has previously demonstrated that biofilms are far less susceptible to antibiotic agents than planktonic bacteria (Donlan & Costerton, 2002)(Davies, 2003). Furthermore, it has been recently demonstrated that *Borrelia* biofilms are more resistant to antibiotic and anti-microbial agents than planktonic spirochetes (Theophilus *et al.*, 2015 ; Sapi *et al.*, 2011). As such, reduced spirochete counts and increased biofilm content of *Borrelia* at 37°C might indicate that temperature may indirectly influence the susceptibility of the bacterium to antibiotic and anti-microbial agents by encouraging biofilm phenotype of the bacterium when compared to the planktonic phenotype.

It has previously been demonstrated that temperature can influence the production of extracellular polymeric substance in the biofilms. *Listeria monocytogenes* has altered EPS production at different temperatures (Norwood & Gilmour., 2001 ; Di Bonaventura et al., 2008). Additionally, in bacterium *Bacillus megaterium*, lower growth temperature of 25°C results in lower production of polysaccharides whereas, a greater temperature range of 30°C-35°C reported higher production of polysaccharides (Gandhi *et al.*, 1998). In *Staphylococcus epidermis* extracellular polysaccharides have been demonstrated to play an important role in cell-cell adhesion and forming multiple layers in the biofilm (Cramton *et al.*, 1999). In bacteria *Pseudomonas aeruginosa* extracellular polysaccharides are responsible for providing cell-cell interaction, primary structural scaffold for the biofilm, surface adherence and maintenance of the biofilm architecture (Ma *et al.*, 2009)(Colvin *et al.*, 2011). In this study, we not only demonstrate enhanced carbohydrate content (μg) present per μm^2 of the biofilm but also an increase in the amount of biofilms produced at 37°C in comparison to 23°C and 33°C. Therefore, the findings of this study strongly suggest that

temperature may play an important role in modulating the production of extracellular polysaccharide content within the biofilms which may in-turn lead to increased biofilm formation.

EPS plays an important role in biofilm formation, adhesion and anchorage, as demonstrated in several bacteria (Norwood & Gilmour, 2001 ; Orgad *et al.*, 2011 ; Ahimou *et al.*, 2007 ; Vu *et al.*, 2009 ; Tielen *et al.*, 2005). Biofilms undergo changes in their stress response properties due to polysaccharides turning into a gel-like substance, whose strength gradually increases with increase in temperature until reaching a critical point (Villain-Simonnet *et al.*, 2000). The altered biofilm viscosity may promote substrate adherence, thereby leading to increased biofilm formation (Garrett *et al.*, 2008), as observed in marine *Pseudomonads* (Fletcher, 1977). For instance, bacteria such as *Pseudomonas aeruginosa* can produce polysaccharide alginate which can alter biofilm viscosity and also plays an important role in biofilm adhesion (Hanlon *et al.*, 2001 ; Orgad *et al.*, 2011). In this study, we have demonstrated the presence of alginate as well as mannose in *B. burgdorferi* biofilms at 23°C, 33°C and 37°C. Alginate in *Pseudomonas aeruginosa* provides protection to the biofilm from the surrounding environment, host immune system and antibiotics (Boyd & Chakrabarty, 1995) (Leid *et al.*, 2005) (Cotton *et al.*, 2009). However, some studies have argued that while alginate does have an effect on *Pseudomonas aeruginosa* biofilm development and architecture, it plays a non-essential role in biofilm formation (Stapper *et al.*, 2004). *Pseudomonas aeruginosa* also consists of mannose as a part of its PSL extracellular polysaccharide matrix which assists in bacterial attachment to a surface and also acts like a structural scaffold in mature biofilms (Colvin *et al.*, 2012).

Here, we also demonstrated the presence of extracellular DNA (eDNA) in *Borrelia* biofilms at 23°C and 37°C in addition to 33°C as described previously (Sapi *et al.*, 2012 ; Timmaraju et al., 2015). Extracellular DNA in bacteria such as *Pseudomonas aeruginosa*, *Staphylococcus epidermis* and *Streptococcus mutans* LT11 promotes biofilm formation by aiding the initial attachment of the bacterial cells to the substratum (Das *et al.*, 2011 ; Qin *et al.*, 2007 ; Whitchurch *et al.*, 2002). In *Pseudomonas aeruginosa*, Psl polysaccharides physically interact with the extracellular DNA to form extracellular DNA-Psl fibers that give a structural framework for biofilm growth and protect the biofilm against EPS targeting agents (Wang *et al.*, 2015). Furthermore, extracellular DNA and alginate have been shown to collectively provide resistance to *Pseudomonas aeruginosa* against Gentamicin (Aspe & Jensen, 2012). While resistance to antibiotics and anti-microbial agents has been demonstrated by *B. burgdorferi* biofilms, the role of extracellular polymeric substance such as alginate, mannose and eDNA in conferring resistance to *Borrelia* biofilms against these agents is yet to be determined (Theophilus *et al.*, 2015 ; Sapi *et al.*, 2011). Bacteria such as *Enterococcus faecalis* has demonstrated a robust biofilm formation even after the eDNA release mechanism in the bacterium was impaired by using proteins as cell surface adhesins and essential matrix components for biofilms formation (Iyer & Hancock, 2012). Increased biofilm quantity and reduced extracellular DNA content (µg) present per μm^2 of the biofilm at 37°C for strain B31 suggests that extracellular DNA might not be essential for robust biofilm formation at 37°C *in vitro*.

Instances of temperature effecting biofilm morphology have been reported in bacteria such as *Legionella Pneumophila* which forms filamentous mat-like biofilms at 37^0C and 42^0C, while at 25^0C the biofilm consisted of rod shaped planktonic cells (Piao *et al.*, 2006). However, we did not observe any significant differences in morphology and nanotopography of the biofilms, and observed tower morphology of *Borrelia* biofilms at all three temperatures, as described previously

(Timmaraju *et al.,* 2015). Tower shaped morphology of biofilms has been observed in *Pseudomonas aeruginosa* and *Staphylococcus aureus* (Cowan *et al.*, 2000) (Moormeier et al., 2014). In *Staphylococcus aureus* distinct and focused biofilm growth was reported after inoculation, resulting in the formation of biofilm towers (Moormeier et al., 2014). Tower shaped morphology of biofilms at all three temperatures suggests that unlike other bacteria, temperature does not alter the development of *Borrelia* biofilms

Strain specific differences have been observed in the amount of biofilms produced, biofilm morphology and the EPS polysaccharides observed in various bacteria such as *Pseudomonas aeruginosa, Listeria monocytogenes* and *E. coli* (Allegrucci & Sauer, 2007 ; Borucki *et al.*, 2003 ; Weiss-Muszkat *et al.*, 2010). For instance, in *Listeria monocytogenes* increased formation of biofilms was observed in strains not responsible for food borne outbreaks when compared to strains known to cause food borne outbreaks (Borucki *et al.*, 2003). *B. burgdorferi* has also demonstrated differences in the amount of biofilm formed, EPS polysaccharides produced between strain B31 and 297 at 37^0C. We observed that at 37^0C, strain B31 forms more biofilms but has reduced EPS polysaccharide production in the biofilms when compared to strain 297. It is interesting to note that strain B31 was isolated from tick *Ixodes dammini* and strain 297 was isolated from human cerebrospinal fluid and the site of strain isolation could have an impact on biofilm formation (Johnson *et al*., 1984). Strain specific differences in biofilm formation have been demonstrated in bacteria such as *Staphylococcus aureus, Acinetobacter baumannii, Pseudomonas aeruginosa, Klebsiella pneumonia* and *Escherichia coli* based on the site of strain isolation (Sanchez *et al.*, 2013). Strains isolated from non-fluid tissues, patients with persistent infection and multi-drug resistant strains are more frequent biofilm formers (Sanchez *et al.*, 2013).

Taken together, mammalian physiological temperature may provide a suitable niche for *B. burgdorferi* biofilm formation. Further studies need to be conducted to demonstrate how temperature influences *Borrelia* biofilm formation and the significance of biofilm formation with regards to the virulence or transmission of bacterium as reported previously in *Yersinia Pestis, Vibrio Cholerae, Pseudomonas aeruginosa, Staphylococcus epidermis* and *Klebsiella pneumonia* (Faruque *et al.*, 2006 ; Hinnebusch & Erickson, 2008 ; Donlan, 2001)

Author contributions

SS, JT, KS and PAST performed the experiments. SS, AT and ES designed the study, interpreted the data and wrote the manuscript.

Acknowledgements

This study was supported by the University of New Haven and grants from the Lymedisease.org, Tom Crawford's Leadership Children's Foundation, Midwest Lyme Foundation, National Philanthropic Trust and Wartman Family to ES and an anonymous donor-advised fund of the NH Charitable Foundation to PAST. Microscopes used in this study were donated to the University of New Haven Lyme Disease Research Group by Lymedisease.org, Schwartz research foundation, Lyme Disease Association and Global Lyme Alliance. The authors thank Dr. Gerald B. Pier (Harvard University) for kindly donating the anti-alginate antibody.

References

Aberer, E. & Duray, P. H. (1991). Morphology of Borrelia burgdorferi: Structural patterns of cultured borreliae in relation to staining methods. *J Clin Microbiol* **29**, 764–772.

Ahmed, N. A. A. M., Petersen, F. C. & Scheie, A. A. (2008). Biofilm formation and autoinducer-2 signaling in *Streptococcus intermedius*: Role of thermal and pH factors. *Oral Microbiol Immunol* **23**, 492–497.

Ahimou, F., Semmens, M. J., Haugstad, G. & Novak, P. J. (2007). Effect of protein, polysaccharide, and oxygen concentration profiles on biofilm cohesiveness. *Appl Environ Microbiol* **73**, 2905–2910.

Alban, P. S., Johnson, P. W. & Nelson, D. R. (2000). Serum-starvation-induced changes in protein synthesis and morphology of Borrelia burgdorferi. *Microbiology* **146 Pt 1**, 119–27.

Allegrucci, M. & Sauer, K. (2007). Characterization of colony morphology variants isolated from Streptococcus pneumoniae biofilms. *J Bacteriol* **189**, 2030–2038.

Al-Robaiy, S., Dihazi, H., Kacza, J., Seeger, J., Schiller, J., Huster, D., Knauer, J. & Straubinger, R. K. (2010). Metamorphosis of Borrelia burgdorferi organisms--RNA, lipid and protein composition in context with the spirochetes' shape. *J Basic Microbiol* **50 Suppl 1**, S5–17.

Angeles-morales, E., Mondragón-flores, R., Luna-arias, J., Enríquez-nieto, C., Parra-ortega, B. & Castro-escarpulli, G. (2012). Evaluation of Morphological Changes of Aeromonas caviae Sch3 Biofilm Formation under Optimal Conditions. *Adv Microbiol* **1**, 552–560.

Aspe, M. & Jensen, L. (2012). The Role of Alginate and Extracellular DNA in Biofilm-Meditated Pseudomonas aeruginosa Gentamicin Resistance. *J Exp Microbiol Immunol* **16**, 42–48.

Barbour, A. G. & Hayes, S. F. (1986). Biology of Borrelia species. *Microbiol Rev* **50**, 381–400.

Borucki, M. K., Peppin, J. D., White, D., Loge, F. & Call, D. R. (2003). Variation in biofilm formation among strains of *Listeria monocytogenes*. *Appl Environ Microbiol* **69**, 7336–7342.

Brisson, D., Vandermause, M. F., Meece, J. K., Reed, K. D. & Dykhuizen, D. E. (2010). Evolution of northeastern and midwestern *Borrelia burgdorferi*, United States. *Emerg Infect Dis* **16**, *911–917.*

Boyd, A. & Chakrabarty, A. M. (1995). Pseudomonas aeruginosa biofilms: Role of the alginate exopolysaccharide. *J Ind Microbiol* **15**, 162-168

Colvin, K. M., Gordon, V. D., Murakami, K., Borlee, B. R., Wozniak, D. J., Wong, G. C. L. & Parsek, M. R. (2011). The pel polysaccharide can serve a structural and protective role in the biofilm matrix of Pseudomonas aeruginosa. *PLoS Pathog* **7**, e1001264.

Colvin, K. M., Irie, Y., Tart, C. S., Urbano, R., Whitney, J. C., Ryder, C., Howell, P. L., Wozniak, D. J. & Parsek, M. R. (2012). The Pel and Psl polysaccharides provide Pseudomonas aeruginosa structural redundancy within the biofilm matrix. *Environ Microbiol* **14**, 1913–1928.

Cotton, L., Graham, R. & Lee, R. (2009). The role of alginate in P. aeruginosa PAO1 biofilm

structural resistance to gentamicin and ciprofloxacin. *J Exp Microbiol Immunol* **13**, 58–62.

Cowan, S. E., Gilbert, E., Liepmann, D. & Keasling, J. D. (2000). Commensal interactions in a dual-species biofilm exposed to mixed organic compounds. *Appl Environ Microbiol* **66**, 4481–4485.

Cramton, S. E., Gerke, C., Schnell, N. F., Nichols, W. W. & Gotz, F. (1999). The Intercellular Adhesion (ica) Locus Is Present in *Staphylococcus aureus* and Is Required for Biofilm Formation. *Infect Immun* **67**, 5427–5433.

Czaczyk, K. & Myszka, K. (2007). Biosynthesis of extracellular polymeric substances (EPS) and its role in microbial biofilm formation. *Polish J Environ Stud* **16**, 799–806.

da Silva Meira, Q. G., de Medeiros Barbosa, I., Alves Aguiar Athayde, A. J., de Siqueira-Júnior, J. P. & de Souza, E. L. (2012). Influence of temperature and surface kind on biofilm formation by Staphylococcus aureus from food-contact surfaces and sensitivity to sanitizers. *Food Control* **25**, 469–475.

Das, T., Sharma, P. K., Krom, B. P., Van Der Mei, H. C. & Busscher, H. J. (2011). Role of eDNA on the adhesion forces between streptococcus mutans and substratum surfaces: Influence of ionic strength and substratum hydrophobicity. *Langmuir* **27**, 10113–10118.

Di Bonaventura, G., Piccolomini, R., Paludi, D., D'Orio, V., Vergara, A., Conter, M. & Ianieri, A. (2008). Influence of temperature on biofilm formation by *Listeria monocytogenes* on various food-contact surfaces: Relationship with motility and cell surface hydrophobicity. *J Appl Microbiol* **104**, 1552–1561.

Donlan, R. M. (2001). Biofilms and device-associated infections. In *Emerg Infect Dis*, **7(2)**. 277–281.

Donlan, R. M. & Costerton, J. W. (2002). Biofilms: Survival mechanisms of clinically relevant microorganisms. *Clin Microbiol Rev* **15**, 167–193.

Dunham-Ems, S. M., Caimano, M. J., Pal, U., Wolgemuth, C. W., Eggers, C. H., Balic, A. & Radolf, J. D. (2009). Live imaging reveals a biphasic mode of dissemination of Borrelia burgdorferi within ticks. *J Clin Invest* **119**, 3652–3665.

Dutta, D. & Willcox, M. (2013). A laboratory assessment of factors that affect bacterial adhesion to contact lenses. *Biology* (Basel) **2**, 1268–1281.

Embers, M. E., Barthold, S. W., Borda, J. T., Bowers, L., Doyle, L., Hodzic, E., Jacobs, M. B., Hasenkampf, N. R., Martin, D. S. & other authors. (2012). Persistence of Borrelia burgdorferi in Rhesus Macaques following Antibiotic Treatment of Disseminated Infection. *PLoS One* **7**, e29914.

Faruque, S. M., Biswas, K., Udden, S. M. N., Ahmad, Q. S., Sack, D. A., Nair, G. B. & Mekalanos, J. J. (2006). Transmissibility of cholera: In vivo-formed biofilms and their relationship to infectivity and persistence in the environment. *Proc Natl Acad Sci* **103**, 6350–6355.

Feng, J., Wang, T., Shi, W., Zhang, S., Sullivan, D., Auwaerter, P. G. & Zhang, Y. (2014). Identification of novel activity against Borrelia burgdorferi persisters using an FDA approved drug library. *Emerg Microbes Infect* **3**, e49.

Flemming, H. C. & Wingender, J. (2001). Relevance of microbial extracellular polymeric substances (EPSs)--Part I: Structural and ecological aspects. *Water Sci Technol* **43**, 1–8.

Fletcher, M. (1977). The effects of culture concentration and age, time, and temperature on bacterial attachment to polstyrene. *Can J Microbiol* 23, 1–6.Garon, C. F., Doward, D. & M. D, Corwin. (1989). Structural Features of Borrelia Burgdorferi- the Lyme Disease. *Scanning Microsc Int supplement* **3**, 109–115.

Garrett, T. R., Bhakoo, M. & Zhang, Z. (2008). Bacterial adhesion and biofilms on surfaces. *Prog Nat Sci* **18**, 1049–1056.

Gomes-Solecki, M. (2014). Blocking pathogen transmission at the source: reservoir targeted OspA-based vaccines against Borrelia burgdorferi. *Front Cell Infect Microbiol* **4**, 136.

Hanlon, G. W., Denyer, S. P., Olliff, C. J. & Ibrahim, L. J. (2001). Reduction in Exopolysaccharide Viscosity as an Aid to Bacteriophage Penetration through Pseudomonas aeruginosa Biofilms. *Appl Environ Microbiol* **67**, 2746–2753.

Hinnebusch, B. J. & Erickson, D. L. (2008). Yersinia pestis biofilm in the flea vector and its role in the transmission of plague. In *Curr Top Microbiol Immunol*, **322**. 229–248.

Hinthong, W., Indrawattana, N., Pitaksajjakul, P., Pipattanaboon, C., Kongngoen, T., Tharnpoophasiam, P. & Worakhunpiset, S. (2015). Effect of temperature on fimbrial gene expression and adherence of enteroaggregative *Escherichia coli*. *Int J Environ Res Public Health* **12**, 8631–8643.

Høiby, N., Bjarnsholt, T., Givskov, M., Molin, S. & Ciofu, O. (2010). Antibiotic resistance of bacterial biofilms. *Int J Antimicrob Agents* **35**, 322–332.

Johnson, R. C., Schmid, G. P., Hyde, F. W., Steigerwalt, A. G. & Brenner, D. J. (1984). *Borrelia burgdorferi* sp. nov.: Etiologic Agent of Lyme Disease. *Int J Syst Bacteriol* ***34,*** 496–497.

Katsikogianni, M. & Missirlis, Y. F. (2004). Concise review of mechanisms of bacterial adhesion to biomaterials and of techniques used in estimating bacteria-material interactions. *Eur Cells Mater* **8**, 37–57.

Leid, J. G., Willson, C. J., Shirtliff, M. E., Hassett, D. J., Parsek, M. R. & Jeffers, A. K. (2005). The exopolysaccharide alginate protects Pseudomonas aeruginosa biofilm bacteria from IFN-gamma-mediated macrophage killing. *J Immunol* **175**, 7512–7518.

Lewis, K. (2007). Persister cells, dormancy and infectious disease. Nat Rev Microbiol **5**, 48–56.

Ma, L., Conover, M., Lu, H., Parsek, M. R., Bayles, K. & Wozniak, D. J. (2009). Assembly

and development of the Pseudomonas aeruginosa biofilm matrix. *PLoS Pathog* **5**. e1000354.

Miklossy, J., Kasas, S., Zurn, A. D., McCall, S., Yu, S. & McGeer, P. L. (2008). Persisting atypical and cystic forms of Borrelia burgdorferi and local inflammation in Lyme neuroborreliosis. *J Neuroinflammation* **5**, 40.

Merilainen, L., Herranen, A., Schwarzbach, A. & Gilbert, L. (2015). Morphological and biochemical features of Borrelia burgdorferi pleomorphic forms. *Microbiol (United Kingdom)* **161**, 516–527.

Moormeier, D. E., Bose, J. L., Horswill, A. R. & Bayles, K. W. (2014). Temporal and stochastic control of Staphylococcus aureus biofilm development. *MBio* **5**, e01341-14

Norwood, D. E. & Gilmour, A. (2001). The differential adherence capabilities of two Listeria monocytogenes strains in monoculture and multispecies biofilms as a function of temperature. *Lett Appl Microbiol* **33**, 320–324.

O'Toole, G., Kaplan, H. B. & Kolter, R. (2000). Biofilm formation as microbial development. *Annu Rev Microbiol* **54**, 49–79.

Obana, N., Nakamura, K. & Nomura, N. (2014). A sporulation factor is involved in the morphological change of *Clostridium perfringens* biofilms in response to temperature. *J Bacteriol* **196**, 1540–50.

Ochiai, Y., Yamada, F., Mochizuki, M., Takano, T., Hondo, R. & Ueda, F. (2014). Biofilm formation under different temperature conditions by a single genotype of persistent Listeria monocytogenes Strains. *J Food Prot* **77**, 133–40.

Orgad, O., Oren, Y., Walker, S. L. & Herzberg, M. (2011). The role of alginate in Pseudomonas aeruginosa EPS adherence, viscoelastic properties and cell attachment. *Biofouling* **27**, 787–798.

Piao, Z., Sze, C. C., Barysheva, O., Iida, K. I. & Yoshida, S. I. (2006). Temperature-regulated formation of mycelial mat-like biofilms by Legionella pneumophila. *Appl Environ Microbiol* **72**, 1613–1622.

Qin, Z., Ou, Y., Yang, L., Zhu, Y., Tolker-Nielsen, T., Molin, S. & Qu, D. (2007). Role of autolysin-mediated DNA release in biofilm formation of Staphylococcus epidermidis. *Microbiology* **153**, 2083–2092.

Rudenko, N., Golovchenko, M., Grubhoffer, L. & Oliver, J. H. (2011). Updates on Borrelia burgdorferi sensu lato complex with respect to public health. *Ticks Tick Borne Dis* **2**, 123–128.

Sanchez, C. J., Mende, K., Beckius, M. L., Akers, K. S., Romano, D. R., Wenke, J. C. & Murray, C. K. (2013). Biofilm formation by clinical isolates and the implications in chronic infections. *BMC Infect Dis* **13**, 47.

Sapi, E., Kaur, N., Anyanwu, S., Luecke, D. F., Datar, A., Patel, S., Rossi, M. & Stricker, R. B. (2011). Evaluation of in-vitro antibiotic susceptibility of different morphological forms of *Borrelia burgdorferi*. *Infect Drug Resist* **4**, 97–113.

Sapi, E., Bastian, S. L., Mpoy, C. M., Scott, S., Rattelle, A., Pabbati, N., Poruri, A., Burugu, D., Theophilus, P. A. S. & other authors. (2012). Characterization of Biofilm Formation by Borrelia burgdorferi In Vitro. *PLoS One* **7**, e48277.

Sapi, E., Balasubramanian, K., Poruri, A., Maghsoudlou, J. S., Socarras, K. M., Timmaraju, A. V., Filush, K. R., Gupta, K., Shaikh, S. & other authors. (2016). Evidence of in vivo existence of Borrelia biofilm in borrelial lymphocytomas. *Eur J Microbiol Immunol* **6**, 9–24.

Srere, A. (1973). Studies on cell adhesion. Adhesion of baby hamster kidney cells rate of attachment of BHK cells **56**, 659–665.

Srivastava, S. Y. & de Silva, A. M. (2009). Characterization of Borrelia burgdorferi aggregates. Vector Borne Zoonotic Dis **9**, 323–329.

Stepanović, S., Ćirković, I., Mijač, V. & Švabić-Vlahović, M. (2003). Influence of the incubation temperature, atmosphere and dynamic conditions on biofilm formation by Salmonella spp. *Food Microbiol* **20**, 339–343.

Stewart, P. S. & Franklin, M. J. (2008). Physiological heterogeneity in biofilms. Nat Rev Microbiol **6**, 199–210.

Sutherland, I. W. (2001). Biofilm exopolysaccharides: A strong and sticky framework. *Microbiol* **147**, 6-9.

Tielen, P., Strathmann, M., Jaeger, K. E., Flemming, H. C. & Wingender, J. (2005). Alginate acetylation influences initial surface colonization by mucoid Pseudomonas aeruginosa. *Microbiol Res* **160**, 165–176.

Theophilus, P. A. S., Victoria, M. J., Socarras, K. M., Filush, K. R., Gupta, K., Luecke, D. F. & Sapi, E. (2015). Effectiveness of Stevia rebaudiana whole leaf extract against the various morphological forms of Borrelia burgdorferi in vitro. *Eur J Microbiol Immunol* **5**, 1–13.

Timmaraju, A., Theophilus, P. A. S., Balasubramanian, K., Shakih, S., Leucke, D. F. & Sapi, E. (2015). Biofilm formation by Borrelia sensu lato. *FEMS Microbiol Lett*, 1–6.

Villain-Simonnet, A., Milas, M. & Rinaudo, M. (2000). A new bacterial polysaccharide (YAS34). I. Characterization of the conformations and conformational transition. *Int J Biol Macromol* **27**, 65–75.

Vu, B., Chen, M., Crawford, R. J. & Ivanova, E. P. (2009). Bacterial extracellular polysaccharides involved in biofilm formation. *Molecules* **14**, 2535-2554.

Wang, G., van Dam, A. P., Schwartz, I. & Dankert, J. (1999). Molecular typing of Borrelia burgdorferi sensu lato: taxonomic, epidemiological, and clinical implications. *Clin Microbiol Rev* **12**, 633–653.

Wang, S., Liu, X., Liu, H., Zhang, L., Guo, Y., Yu, S., Wozniak, D. J. & Ma, L. Z. (2015). The exopolysaccharide Psl-eDNA interaction enables the formation of a biofilm skeleton in *Pseudomonas aeruginosa*. *Environ Microbiol Rep* 7, 330–340.

Weiss-Muszkat, M., Shakh, D., Zhou, Y., Pinto, R., Belausov, E., Chapman, M. R. & Sela, S. (2010). Biofilm formation by and multicellular behavior of Escherichia coli O55:H7, an atypical enteropathogenic strain. *Appl Environ Microbiol* **76**, 1545–1554.

Whitchurch, C. B., Tolker-Nielsen, T., Ragas, P. C. & Mattick, J. S. (2002). Extracellular DNA required for bacterial biofilm formation. *Science* **295**, 1487.

Yoong, P., Cywes-Bentley, C. & Pier, G. B. (2012). Poly-N-acetylglucosamine expression by wild-type *Yersinia pestis* is maximal at mammalian, not flea, temperatures. *MBio* **3**, e00217–12.

Figure legends

Fig. 1 Analyses of the number of planktonic spirochetes and biofilm adherence of strains B31 and 297 after 7 days of culture at 37^{0}C. *B. burgdorferi* spirochetes were cultured at 23^{0}C, 33^{0}C or 37^{0}C for a period of 7 days. Spirochetes were visualized through SYBR green staining and the biofilms through phase contrast microscopy in strains B31 (a) and 297 (b), scale bar – 100 µm. The mean number of spirochetes per grid (d) and the % of adherent biofilms after shaking (c) were analyzed. Two-way (ANOVA) was performed using uncorrected Fisher LSD test with $P<0.05$ to determine statistical significance between datasets. Representative data are shown as mean ± SD from 9 independent experiments

Fig. 2 Analyses of biofilm formation in *B. burgdorferi* strains B31 and 297 cultured at 37^{0}C. *B. burgdorferi* spirochetes ($5x10^6$ cells) from strains B31 (a-c) and 297 (d-f) were cultured at 23^{0}C, 33^{0}C or 37^{0}C for a period of 7 days. The culture media was removed on day 7 and the phase contrast micrographs of the biofilms were imaged (n=9). Quantitative comparison of the mean biofilm coverage area and mean individual biofilm coverage area of *B. burgdorferi* biofilms formed at the three temperatures by the two strains was performed using two-way ANOVA (panel g and h respectively). Representative data are shown as mean ± SD from 9 independent experiments. Scale bar - 100 µm.

Fig. 3 3D nano-morphology and topography of representative *Borrelia* biofilms at three different temperatures. *B. burgdorferi* spirochetes from strains B31 (a) and 297 (b) were cultured for 7 days at 23^{0}C, 33^{0}C or 37^{0}C. The biofilms were scanned using SHOCONG probes and Nanosurf eyescan 2 software and the data was analyzed using Gwyddion software. Two dimensional topography profiles of *Borrelia* biofilms of strains B31 (a) and 297 (b) was extracted from AFM scans and plotted using GraphPad.

Fig. 4 Analyses of the height of *B. burgdorferi* biofilms of B31 and 297 strains formed at three different temperatures. *B. burgdorferi* B31 and 297 cells were cultured for 7 days to initiate biofilm formation at 23^{0}C 33^{0}C or 37^{0}C. The culture was removed and the biofilms were analyzed by atomic force microscopy. Mean height of the biofilms was extracted from AFM scans using Gwyddion for 4 random biofilms (n=4) for each strain at three temperatures. Two-way ANOVA using uncorrected Fisher LSD test with significance of $P<0.05$ was performed to determine

statistical variation between the mean heights of the biofilms. Representative data are shown as mean ± SD from 4 independent experiments.

Fig. 5 Presence of alginate, mannose in *Borrelia* biofilms at three different temperatures and increase in the carbohydrate content in biofilms of strains B31 and 297 at 37^{0}C. *B. burgdorferi* biofilms from strain B31 and 297 were cultured at 23^{0}C, 33^{0}C or 37^{0}C for a period of 7 days and stained with 1:100 primary alginate antibody (a) (red) and with polysaccharide mannose specific HHA lectin (b) (green). The biofilms were then counterstained with DAPI (blue, shown in the merge Alginate/DNA and Mannose/DNA). Fluorescent micrographs were acquired using Leica DM 2500 microscope, Scale bar - 100µm. Total carbohydrate content was surmised from triplicates of nine independent experiments (n=9), (c). Total carbohydrate content within the biofilm per µm^2 of the biofilm (µg/µm^2) (d). Two-way ANOVA using uncorrected Fisher LSD multiple comparison test performed with significance P<0.05 was used to determine significant difference between the groups. Representative data are shown as mean ± SD from 9 independent experiments.

Fig. 6 Extracellular DNA content in *Borrelia burgdorferi* biofilm at three different temperature *B. burgdorferi* were cultured at 23^{0}C, 33^{0}C or 37^{0}C for 7 days and then stained with SYBR green dye. Fluorescent micrographs of extracellular DNA staining in the biofilms were acquired using Leica DM 2500 microscope, scale bar = 100µm (a). Mean total extracellular DNA content in the biofilm was obtained from triplicates of three different experiments (n=3) (b). Total extracellular DNA content within the biofilm per µm^2 of the biofilm (µg/µm^2) (c). Two way ANOVA was performed with uncorrected Fisher LSD multiple comparison test, p<0.05 was used to determine statistical significance between the groups. Representative data are shown as mean ± SD from 3 independent experiments.

Fig. S1 Alginate antibody and HHA lectin specificity *B. burgdorferi* biofilms were stained with alginate antibody (1:1000) (c) and HHA lectin (20ng/µl) (g) and counterstained with DAPI (d, h). Inhibition of Alginate antibody (a, b) and HHA lectin (e, f) with sodium alginate (0.05M) and mannose (0.25M) respectively shows the specificity of staining. Fluorescent micrographs were acquired using Leica DM2500 microscope at 400X, scale bar - 100µm.

Fig. S2 Carbohydrate standard curve 1:2 dilutions of Glucose were made to get the concentrations of 16 mg/ml, 8 mg/ml, 4 mg/ml, 2 mg/ml, 1 mg/ml, 0.5 mg/ml, 0.25mg/m, 0.125 mg/ml and 0.0625 mg/ml. TCA assay was performed and the absorbance was measured at 485 nm. Linear regression was performed on absorbance values and goodness of fit R^2 was found to be 0.8810 with p<0.01. Standard deviation of 3 replicates for each concentration is shown.

Fig. S3 Extracellular DNA standard curve Lambda DNA concentrations of 31.25µg/ml, 28.75µg/ml, 26.25µg/ml, 23.75µg/ml, 21.25µg/ml, 18.75µg/ml, 16.25µg/ml and 13.75µg/ml were made and their corresponding fluorescence intensity values were obtained by performing SYBR green DNA quantification assay. Linear regression was performed on the fluorescence intensity values and goodness of fit R^2 was found to be 0.9204 with a p<0.01. Standard deviation of duplicates for each concentration is shown.

643

644

Figure

Click here to download Figure Fig 1.tif

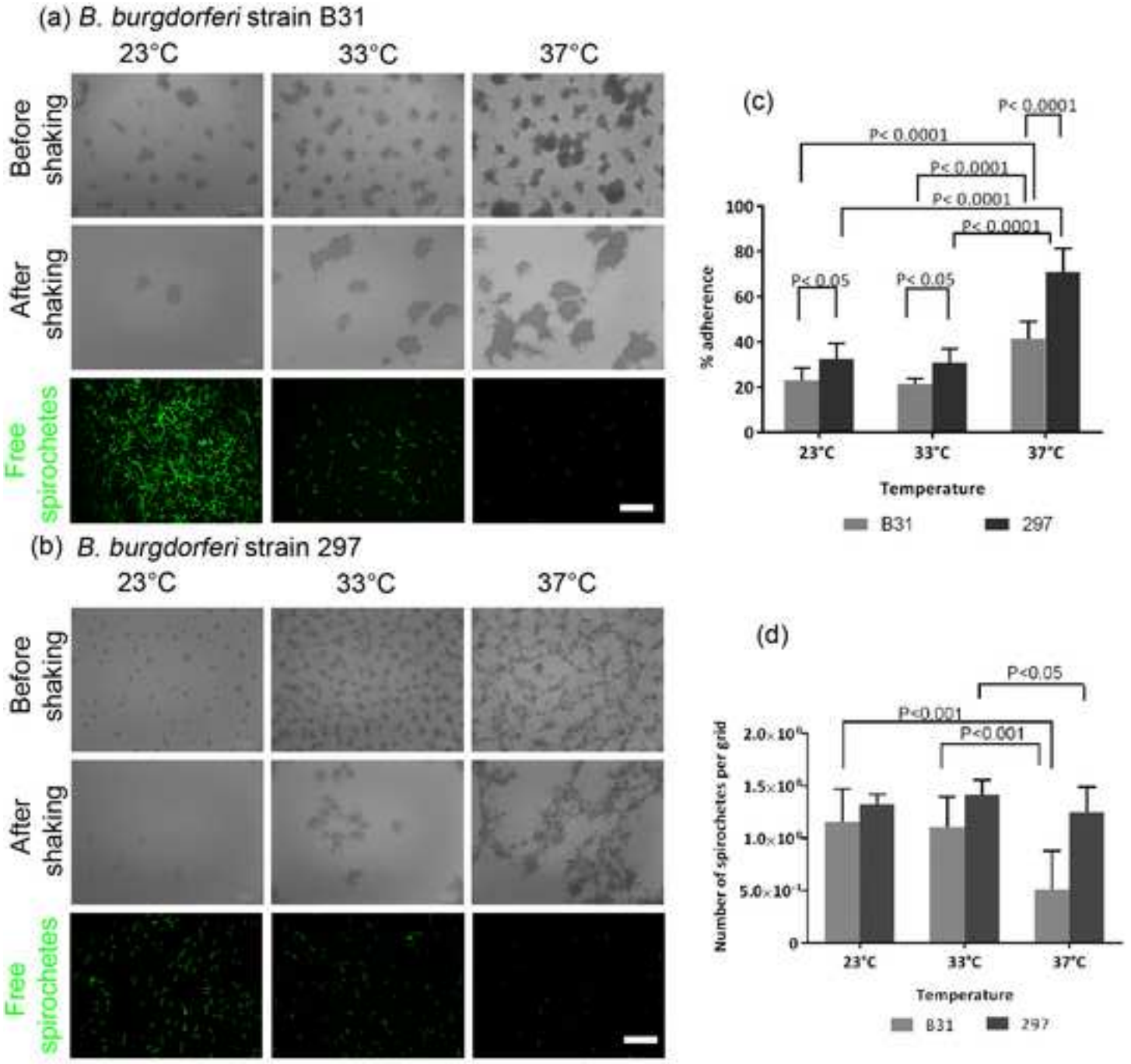

Figure

Click here to download Figure Fig 2.tif

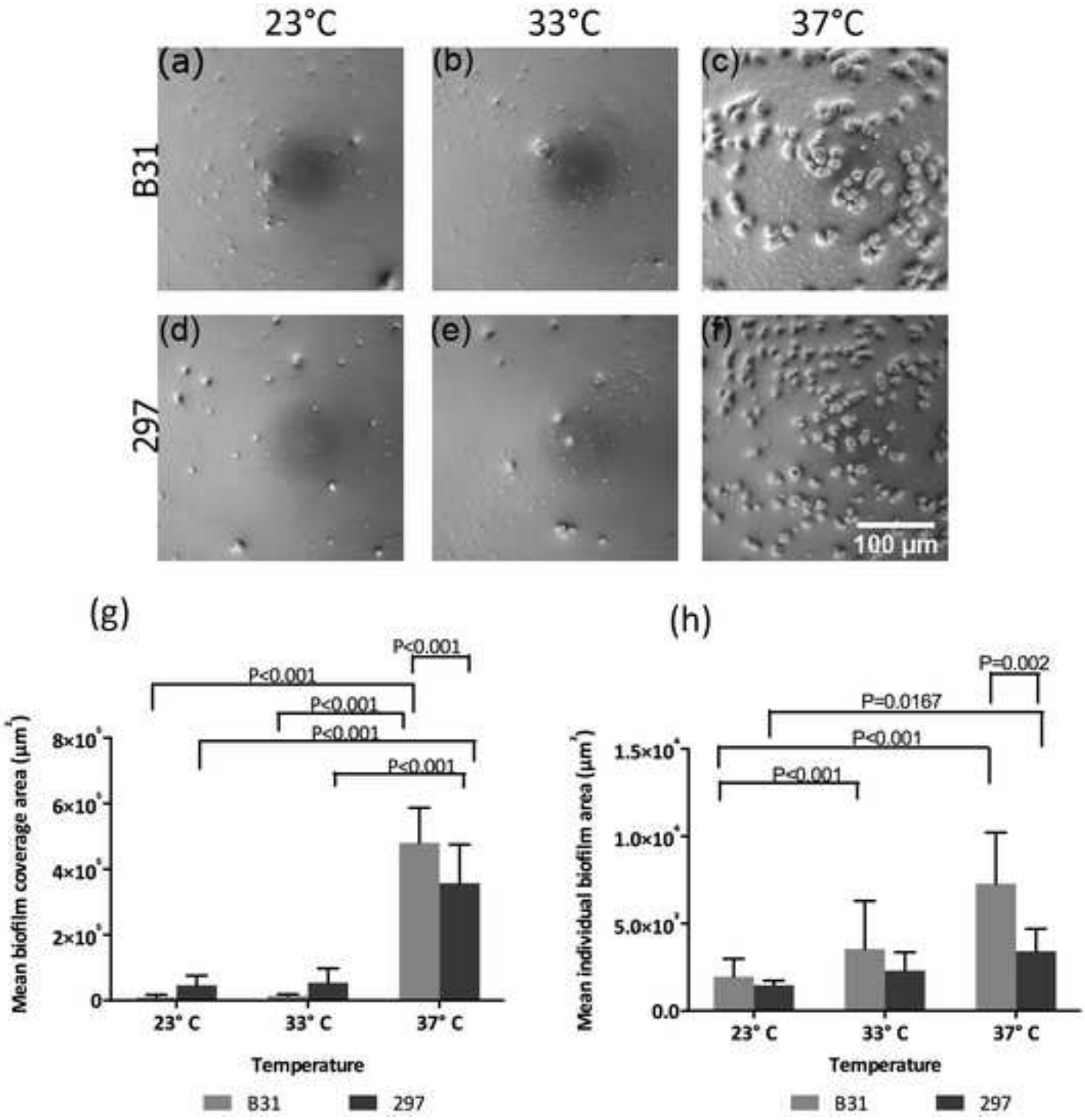

Figure

Click here to download Figure Fig 3.tif

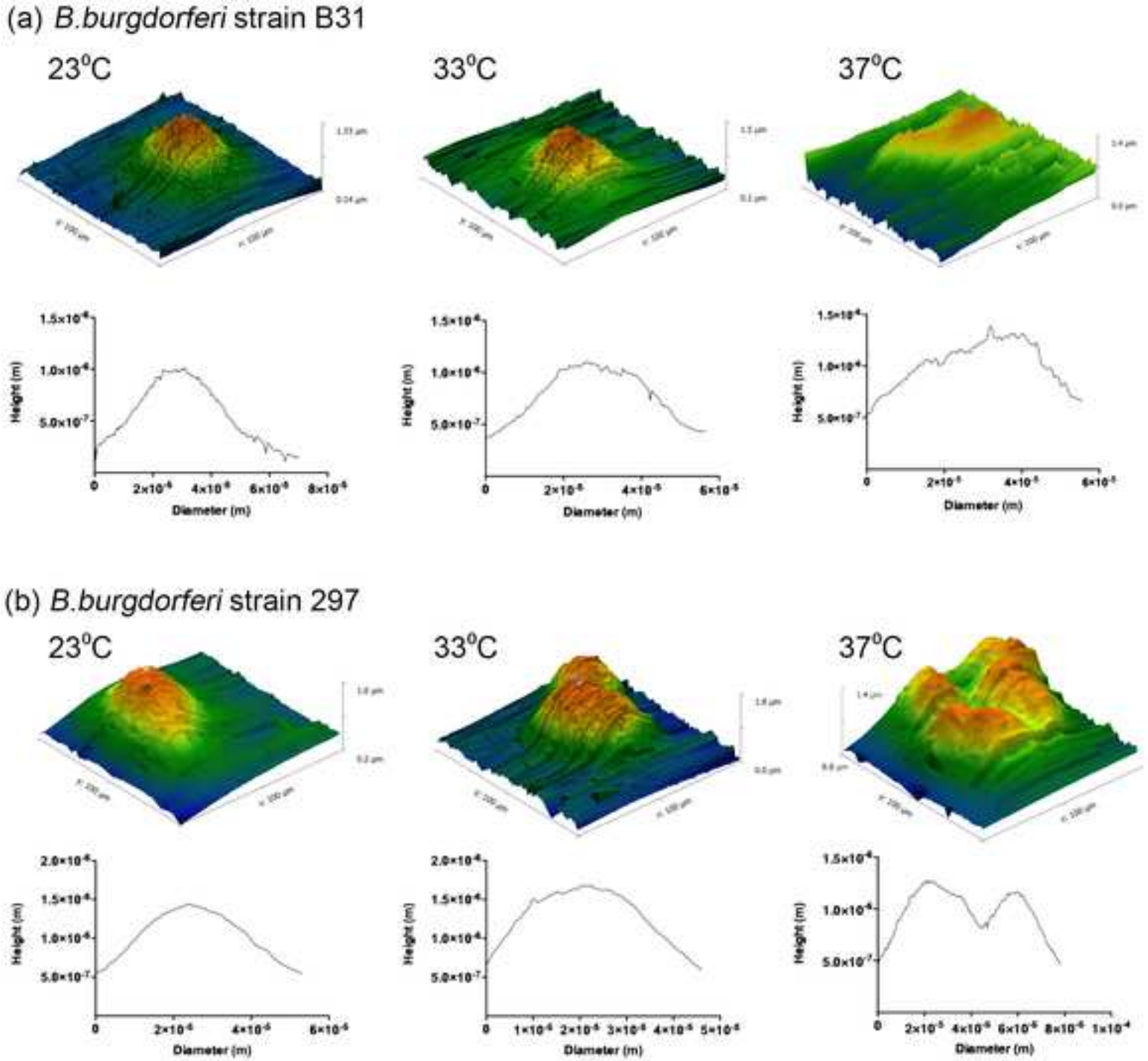

Figure

Click here to download Figure Fig 4.tif

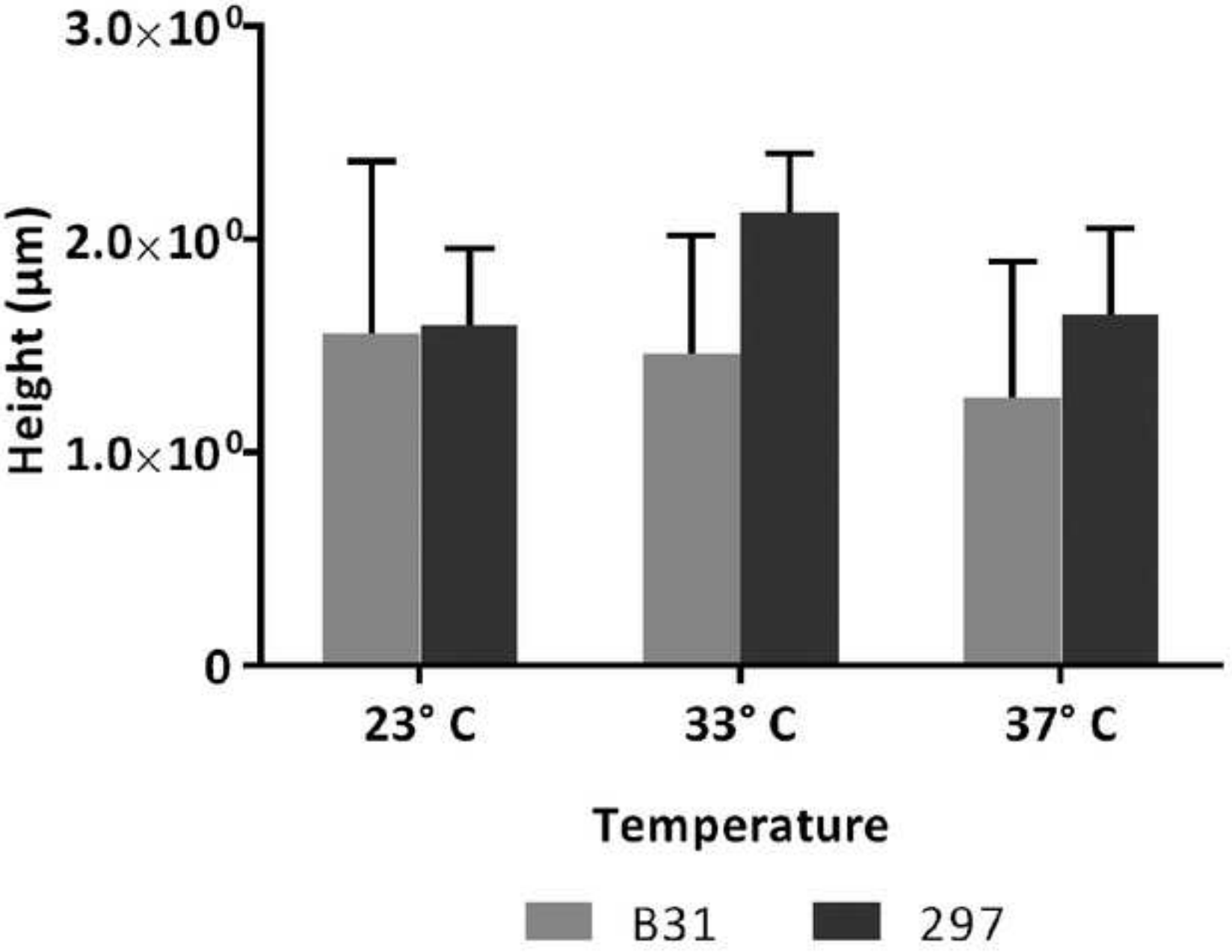

Figure

Click here to download Figure Fig 5.tif

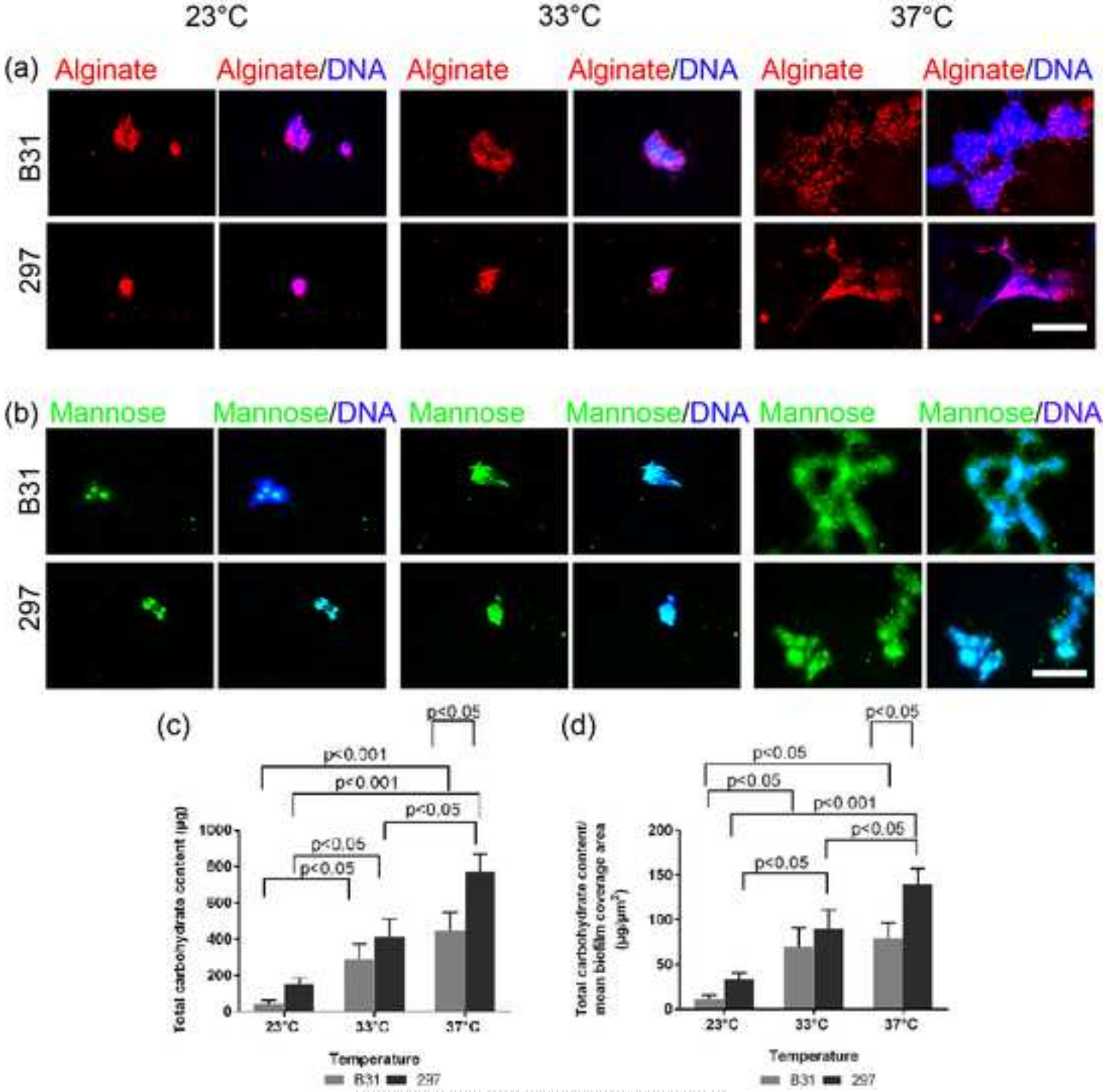

Figure

Click here to download Figure Fig 6.tif

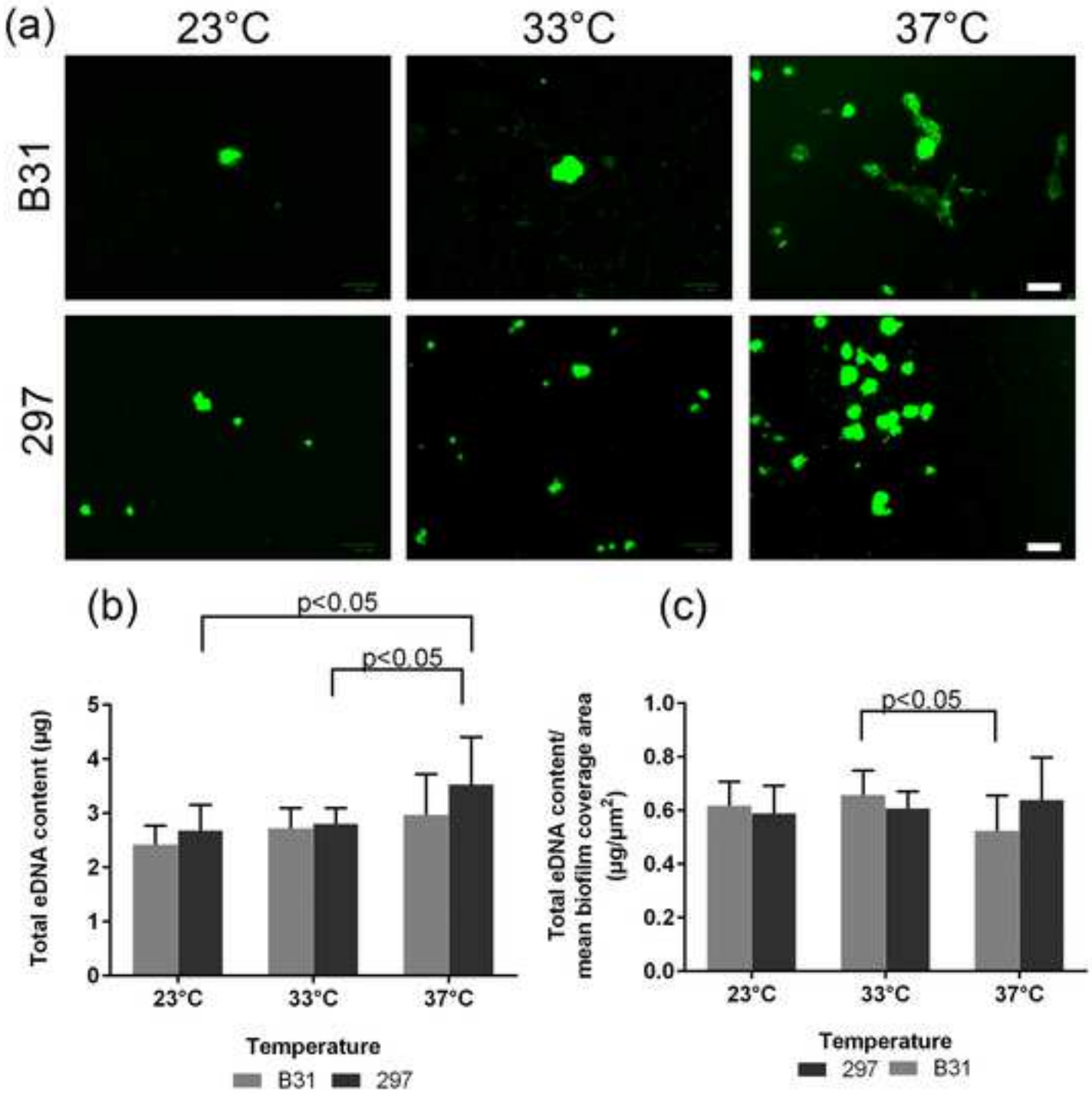

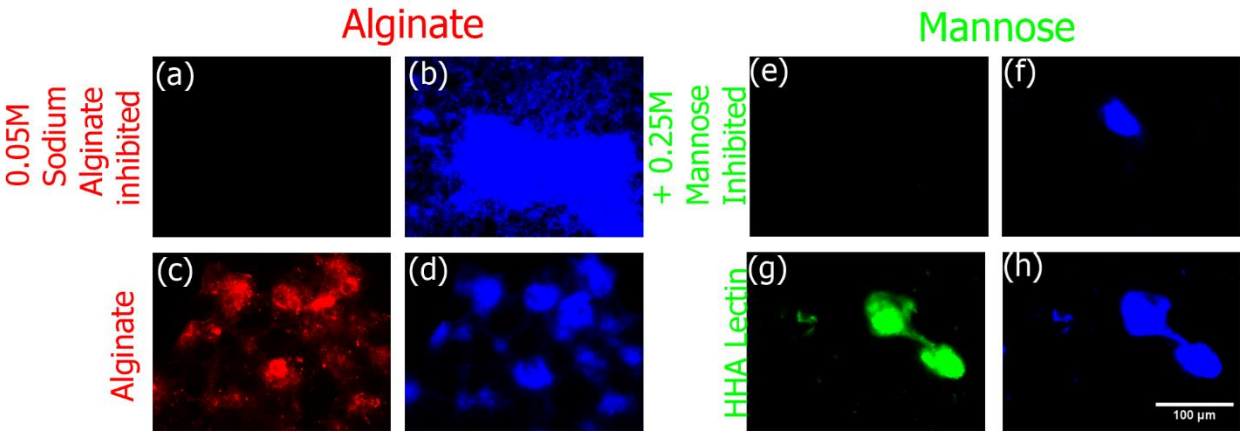

Fig. S1 Alginate antibody and HHA lectin specificity. *B. burgdorferi* biofilms were stained with alginate antibody (1:1000) (c) and HHA lectin (20ng/µl) (g) and counterstained with DAPI (d, h). Inhibition of Alginate antibody (a, b) and HHA lectin (e, f) with sodium alginate (0.05M) and mannose (0.25M) respectively shows the specificity of staining. Fluorescent micrographs were acquired using Leica DM2500 microscope at 400X, scale bar - 100µm.

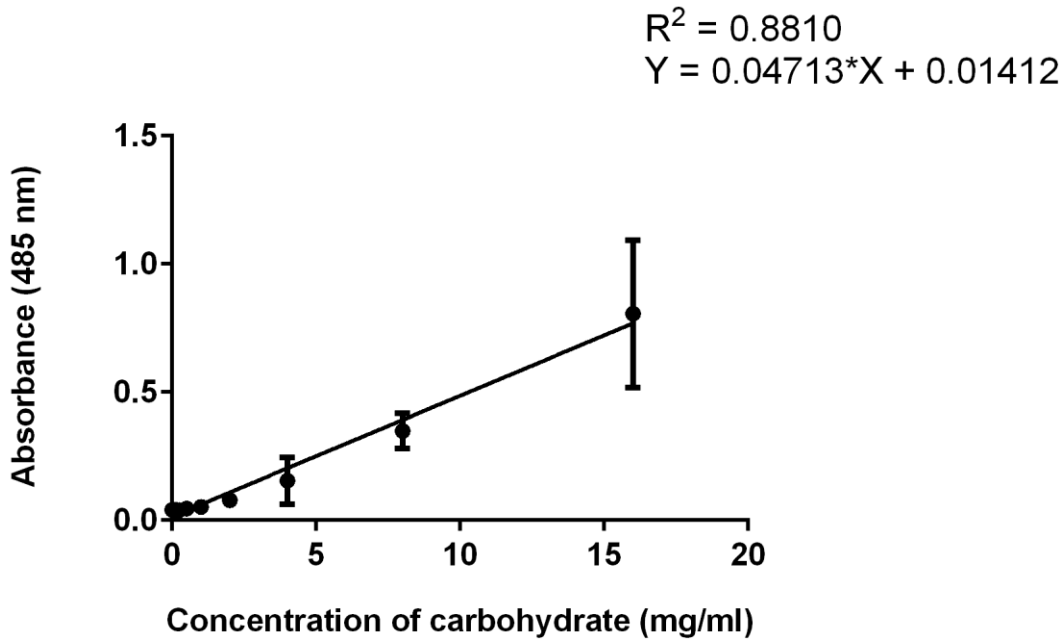

Fig. S2 Carbohydrate standard curve. 1:2 dilutions of Glucose were made to get the concentrations of 16 mg/ml, 8 mg/ml, 4 mg/ml, 2 mg/ml, 1 mg/ml, 0.5 mg/ml, 0.25mg/m, 0.125 mg/ml and 0.0625 mg/ml. TCA assay was performed and the absorbance was measured at 485 nm. Linear regression was performed on absorbance values and goodness of fit R^2 was found to be 0.8810 with $p<0.01$. Standard deviation of 3 replicates for each concentration is shown.

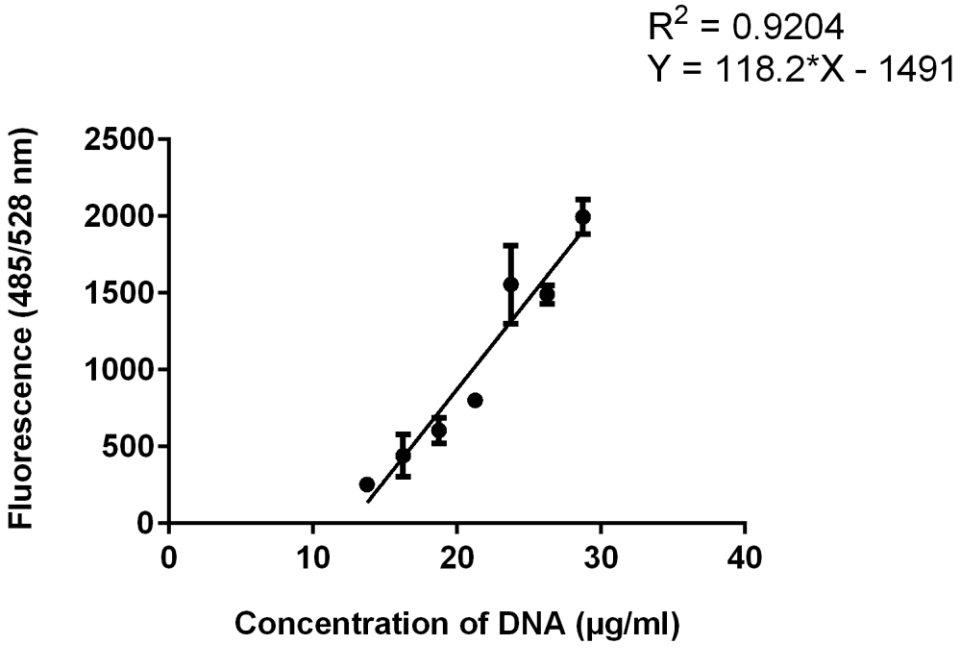

Fig. S3 Extracellular DNA standard curve. Lambda DNA concentrations of 31.25µg/ml, 28.75µg/ml, 26.25µg/ml, 23.75µg/ml, 21.25µg/ml, 18.75µg/ml, 16.25µg/ml and 13.75µg/ml were made and their corresponding fluorescence intensity values were obtained by performing SYBR green DNA quantification assay. Linear regression was performed on the fluorescence intensity values and goodness of fit R^2 was found to be 0.9204 with a $p<0.01$. Standard deviation of duplicates for each concentration is shown.